# Outline



1. Overview of STAR forward calorimetry
2. Physics results: $A_N$ vs. $x_F$
3. Physics results: $A_N$ vs. $p_T$
4. Overview of Forward Meson Spectrometer project
5. High voltage system
6. Electronics and trigger
7. Current status
8. Future highlights

# Forward Pion Detector



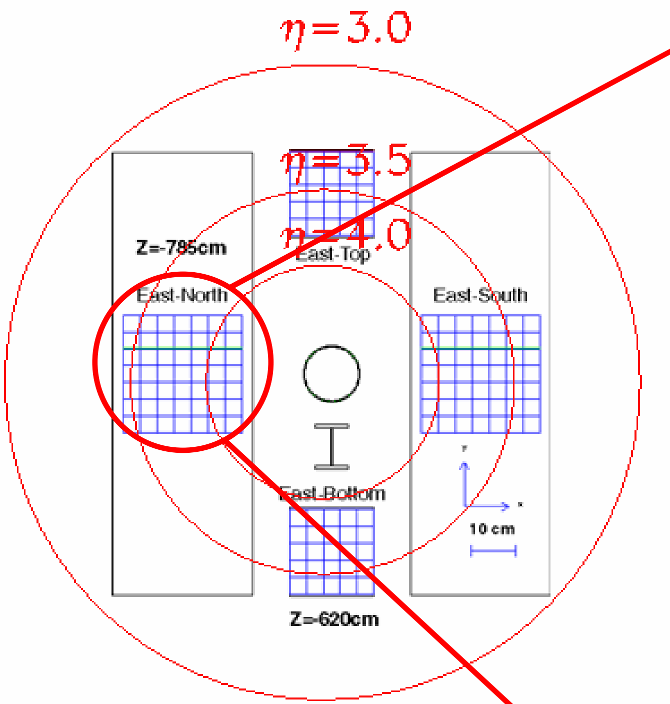


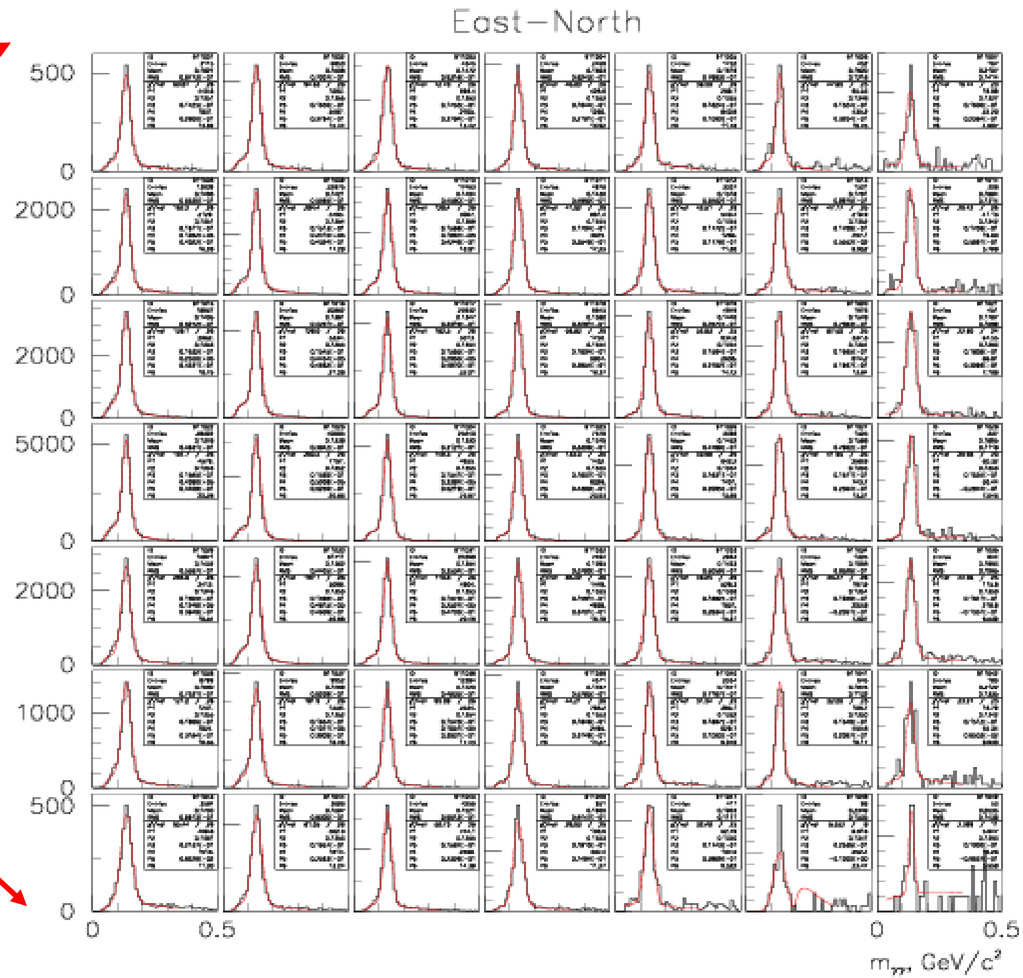


- Two 5x5 arrays of Pb glass cells
- Commissioned on both sides of

# FPD$^{++}$ for Run 6

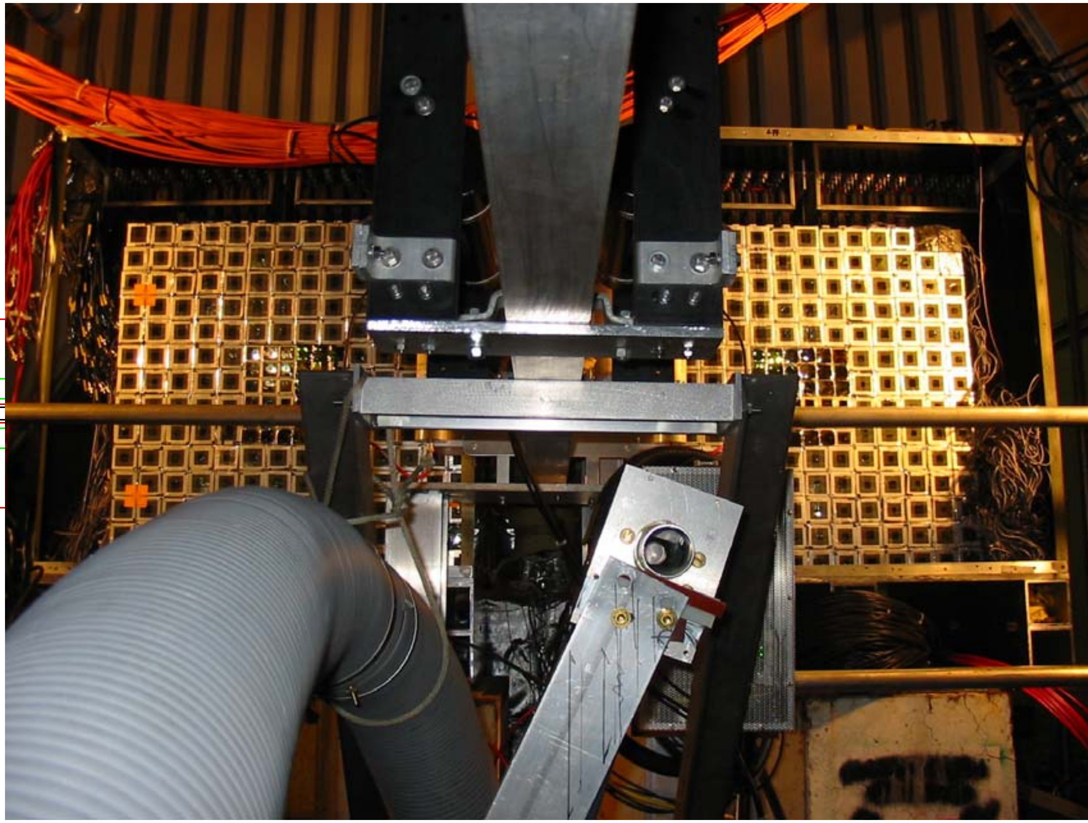

FPD$^{++}$

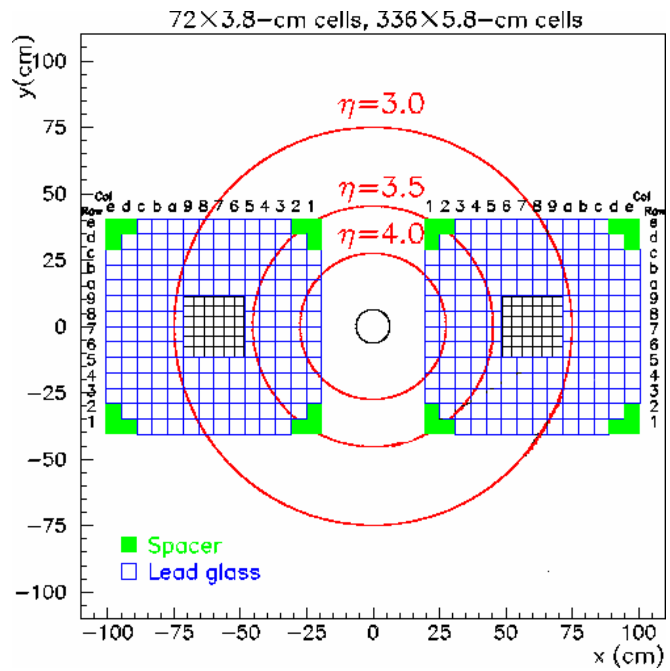


- Expansion of the west FPD
- 6X6 small cells from the FPD at the center + 168 large cells surrounding them.
- Served as a prototype of the ***Forward Meson Spectrometer***

# Acceptance - Run6



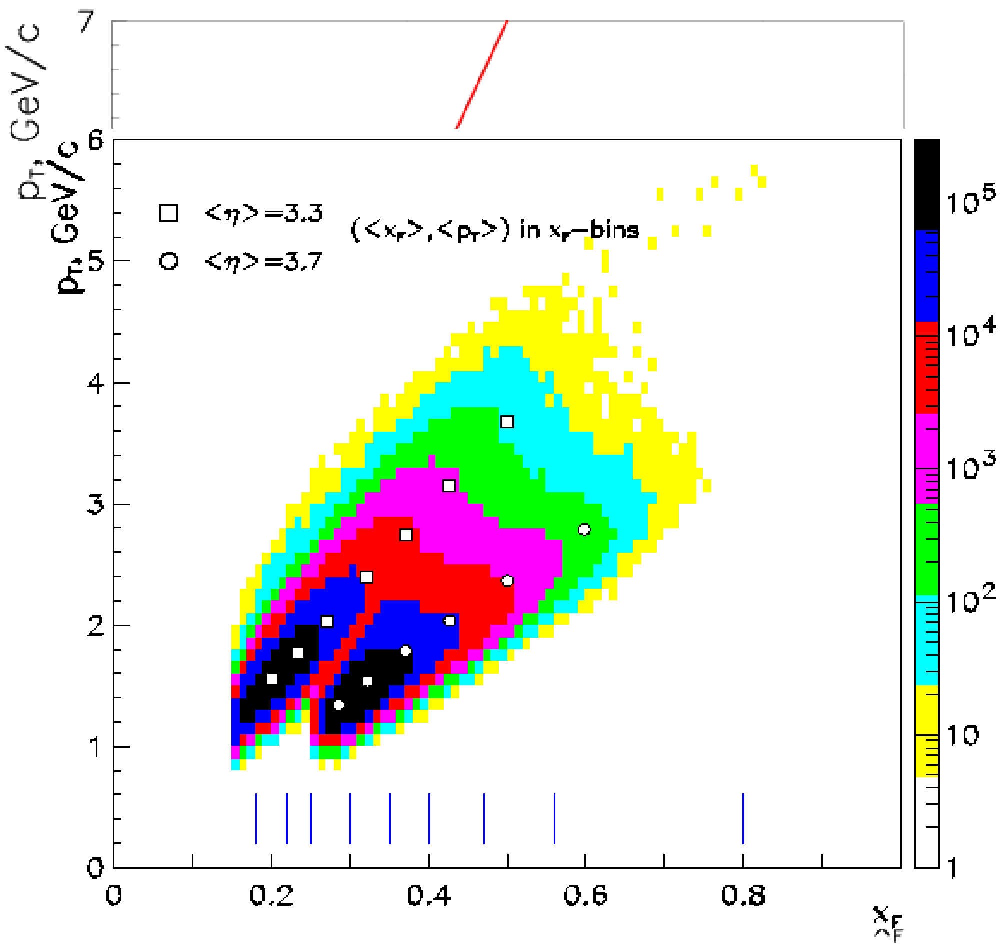


- Limited acceptance for individual detectors → Strong $x_F$ and $p_T$ correlation
- FPD at <η>=3.7 and 4.0, and FPD++ at <η>=3.3. When combined, cover a broad range of $x_F$ and $p_T$
- For given rapidity, event rate falls sharply with both $x_F$ and $p_T$.

# $A_N$ and $\pi^0$ cross section from Run 2



PRL 92, 171801 (2004)

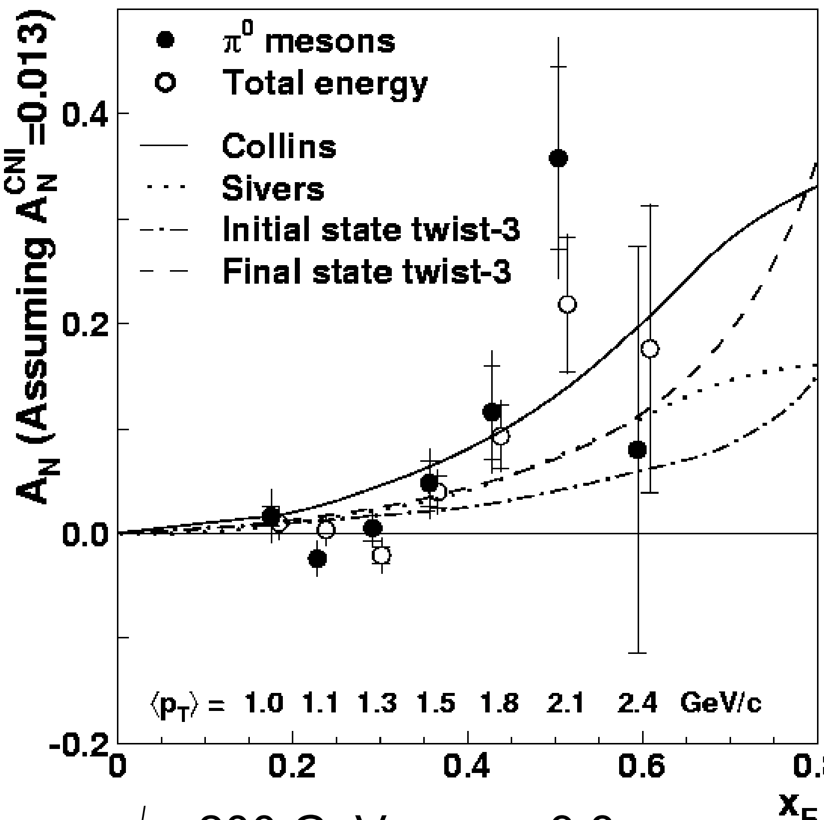


$\sqrt{s}$=200 GeV, <η> = 3.8

Analyzing power vs. $x_F$ for polarized p+p collisions

PRL 97, 152302 (2006)

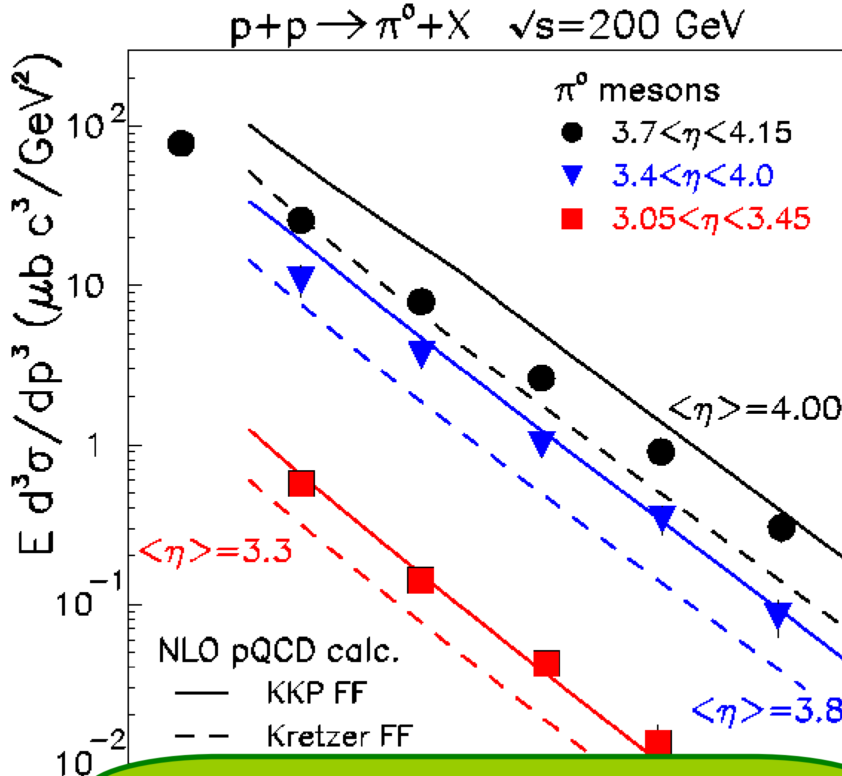


Used in the global analysis of fragmentation function hep-ph/0703242

1. At RHIC energy, $\pi^0$ cross section is consistent with the NLO pQCD calculation
2. Transverse spin asymmetry observed in lower energy persists at RHIC energy

# Transverse Spin Runs at STAR with Forward Calorimetry



| | Run2 | Run3 | Run5 | Run6 |
|---|---|---|---|---|
| detector | EEMC and FPD prototypes | 6 matrices of FPD | full FPD (8 matrices) | ***East FPD West FPD++*** |
| $P_{BEAM}^{\text{sampled}}$, % | ~15 | ~30 | ~45 | ***~60*** |
| $\int Ldt,\ pb^{-1}$ | 0.15 | 0.25 | 0.1 | ***6.8*** |
| $<\eta>$ | 3.8 | ±3.3/±4.0 | ±3.7/±4.0 | ***-3.7/3.3*** |

***Figure of Merit***

***($P_{BEAM}^2$ x L) in Run 6 is ~50 times larger*** *than previous STAR runs combined*

# $x_F$ dependence of $A_N$

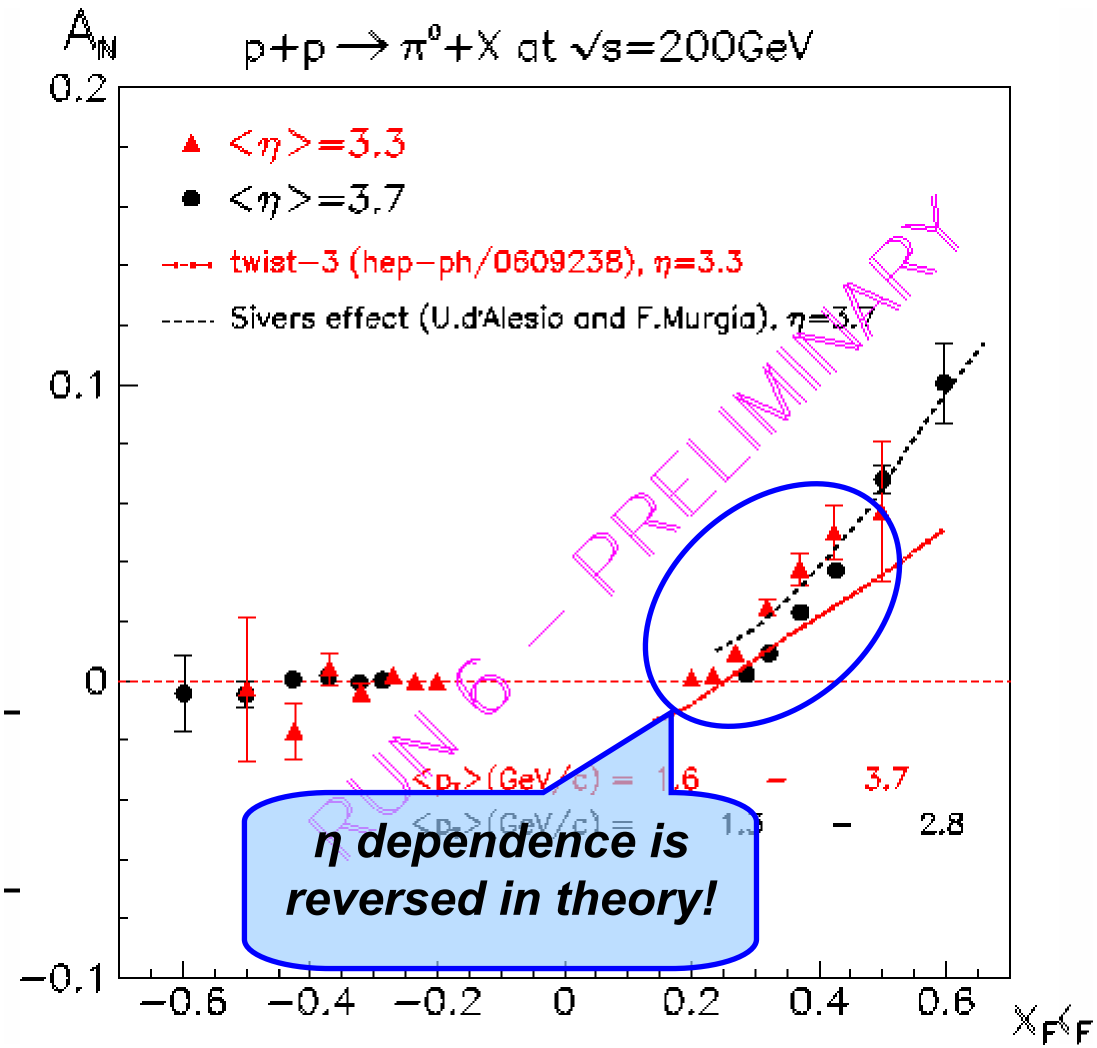


- $A_N$ increases with $X_F$ at positive $x_F$
- $A_N$ is consistent with 0 at negative $x_F$
- Small errors allow quantitative comparison to the theory
- Run 6 added data points at $\eta = 3.3$ → ***The first map of $x_F$ and $p_T$ dependence***

hep-ex/0612030

# $p_T$ dependence of $A_N$ – Theory

Both **Sivers** and **Collins/Heppelmann** models of SSA involves
***$S_T$ dependent $k_T$ offset*** introduced by

- Initial State Parton Distribution Function
→ **Sivers**
- Final State Fragmentation Funcion
→ **Collins/Heppelmann**

$$P_T \Rightarrow P_T \pm k_T$$

$$d\sigma^{\uparrow} \propto \frac{1}{(P_T - k_T)^6} \qquad d\sigma^{\downarrow} \propto \frac{1}{(P_T + k_T)^6}$$

$$A_n \equiv \frac{d\sigma^{\uparrow} - d\sigma^{\downarrow}}{d\sigma^{\uparrow} + d\sigma^{\downarrow}} = \frac{6k_T}{P_T} + O\left(\frac{k_T}{P_T}\right)^2$$

***Falls as $1/P_T$***

Higher Twist effect is ***also suppressed by $p_T$*** as it is required by the definition of higher twist.

**Phys.Rev.D74:114013,2006.**

**$A_N$ vs. $l_T$ from Kouvaris, Qiu, Vogelsang, and Yuan fitted to E704 data**

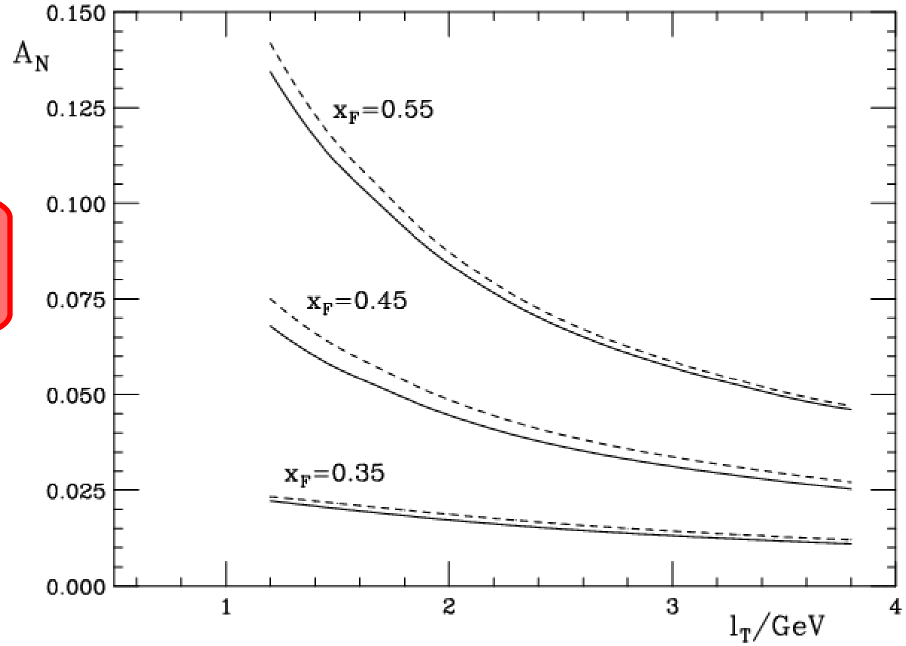

# $p_T$ dependence of $A_N$



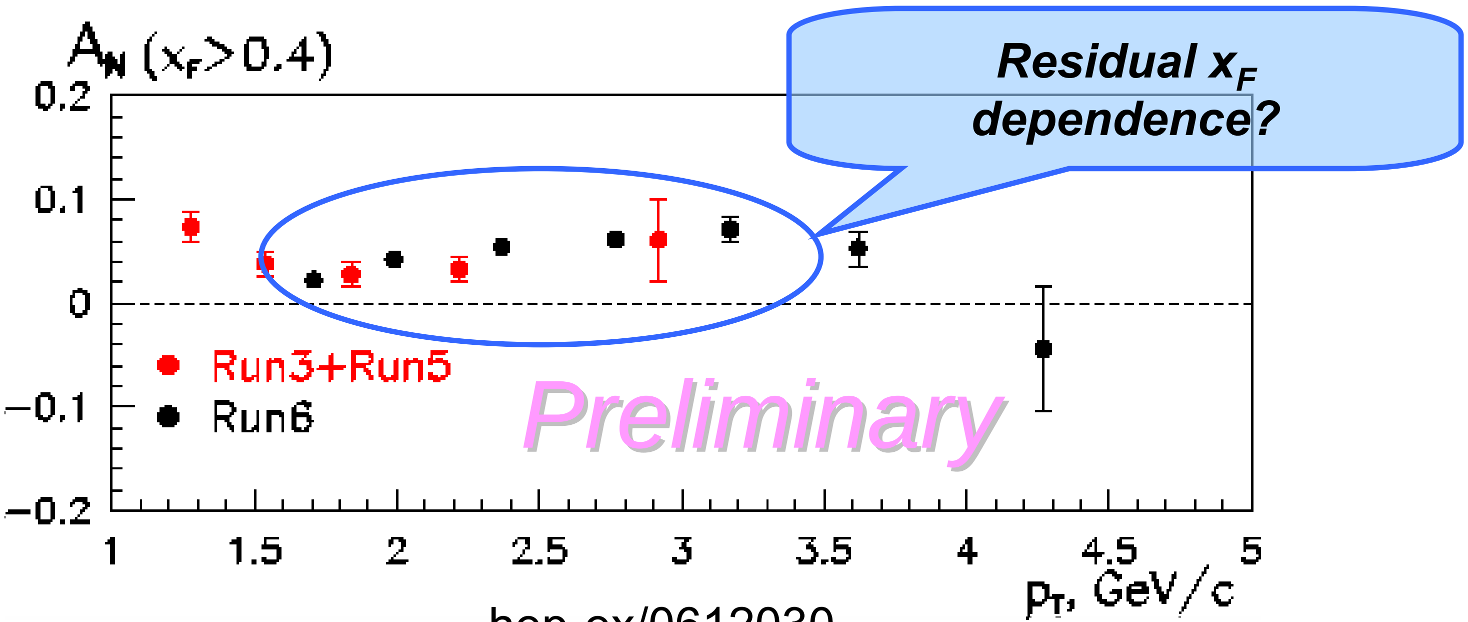


hep-ex/0612030

- Run3 + Run 5 data didn't show an obvious departure from the predicted $1/p_T$ dependence.

- ***With Run6 data added, we see a much more complicated behavior.*** Analyzing power clearly does not fall between ~1.7 GeV and ~3.2 GeV of $p_T$.

# $p_T$ dependence of $A_N$ in $x_F$ bins

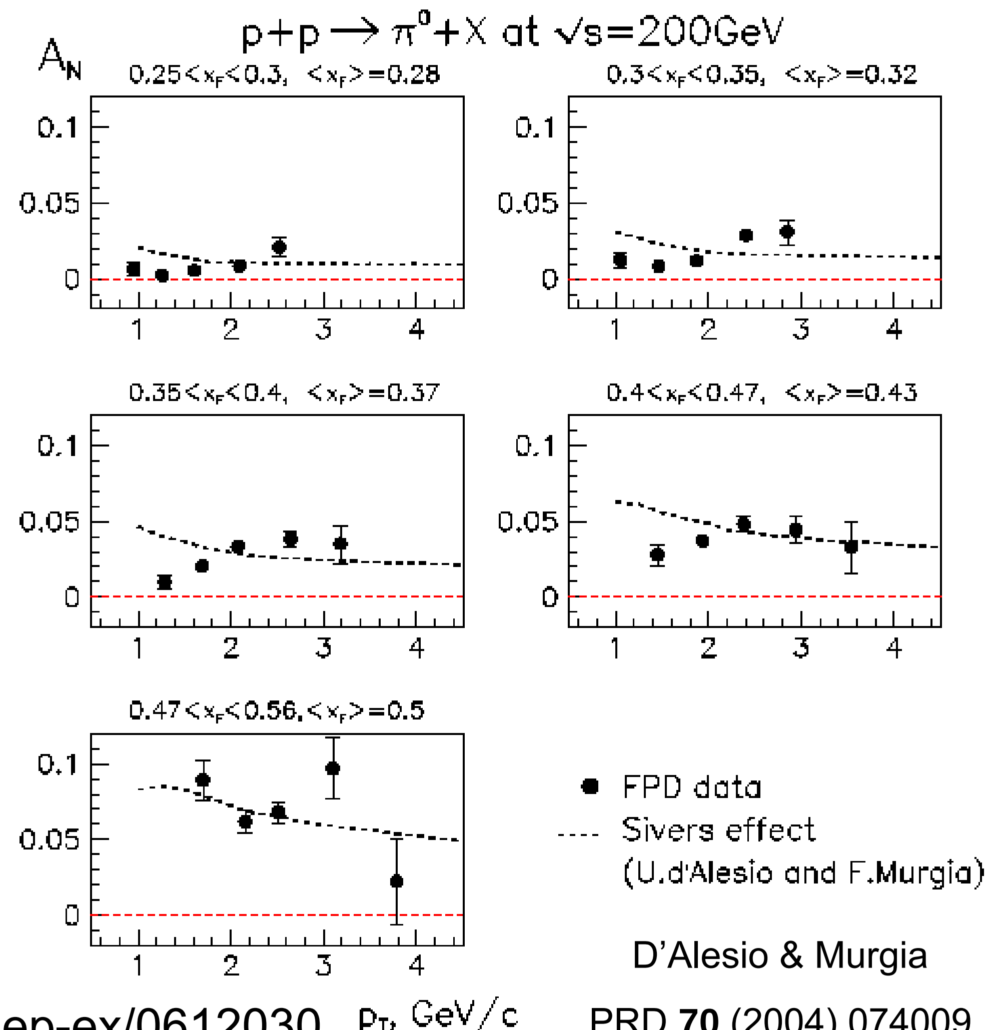


hep-ex/0612030

D'Alesio & Murgia

PRD **70** (2004) 074009

- Combined data from three runs at $<\eta>=3.3$, 3.7 and 4.0
- Within each plot, $x_F$ does not change significantly. → negligible residual $x_F$ dependence.
- ***There is no statistically significant evidence that $A_N$ falls as a function of $p_T$.***

# Forward Meson Spectrometer



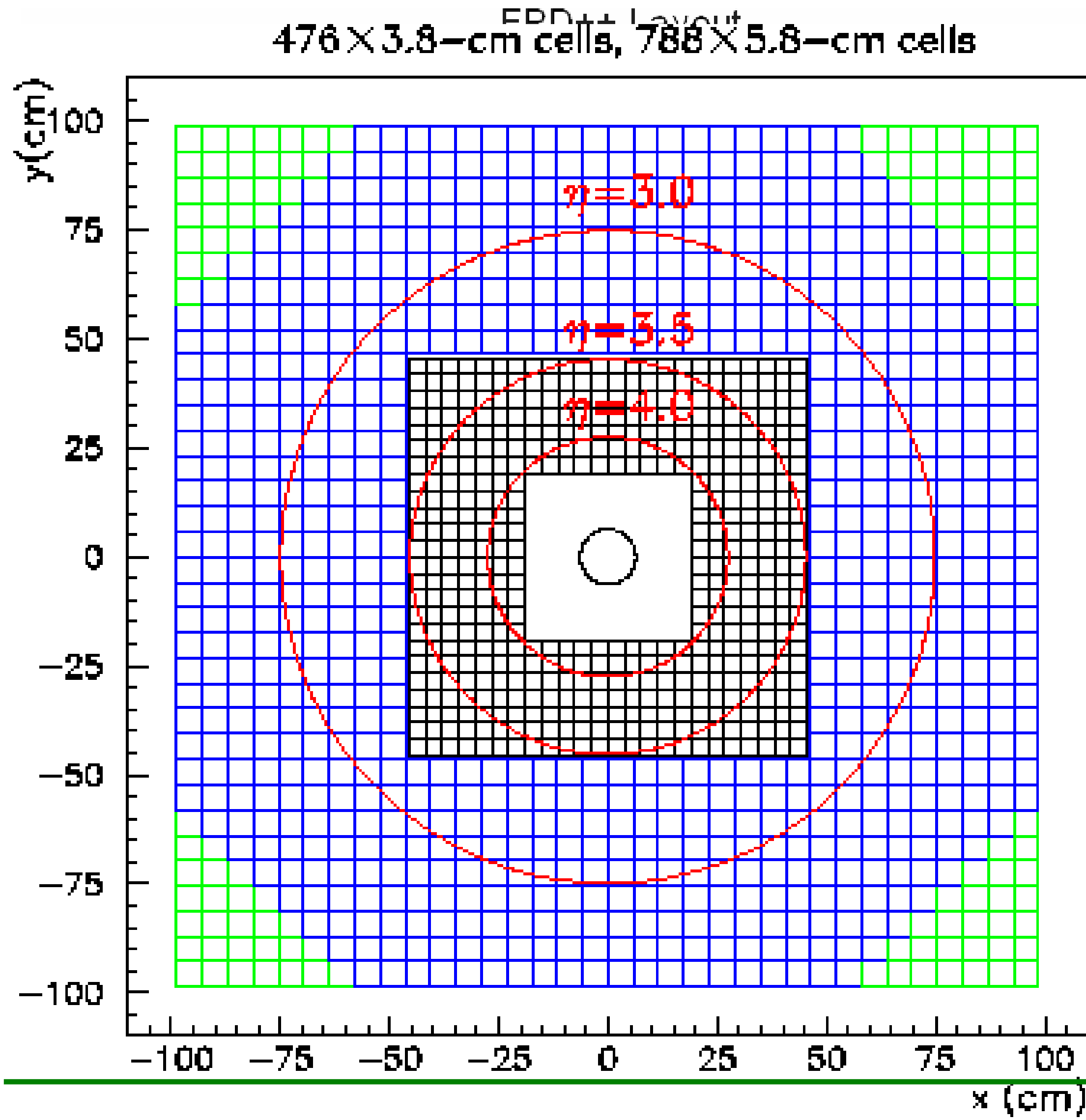


- FMS provides ***full azimuthal coverage for*** $+2.5 \le \eta \le +4$
- Inner calorimeter → 476 small cells, outer calorimeter → 788 large cells.
- Nearside $\pi^0$ pair, Jet-like event reconstruction
  → ***Collins/Heppelmann effect***
- FMS, EEMC and BEMC → awayside jet → ***Sivers effect***
- Large acceptance improves background rejection in ***prompt photon measurement***

# Improved STAR E-M Coverage

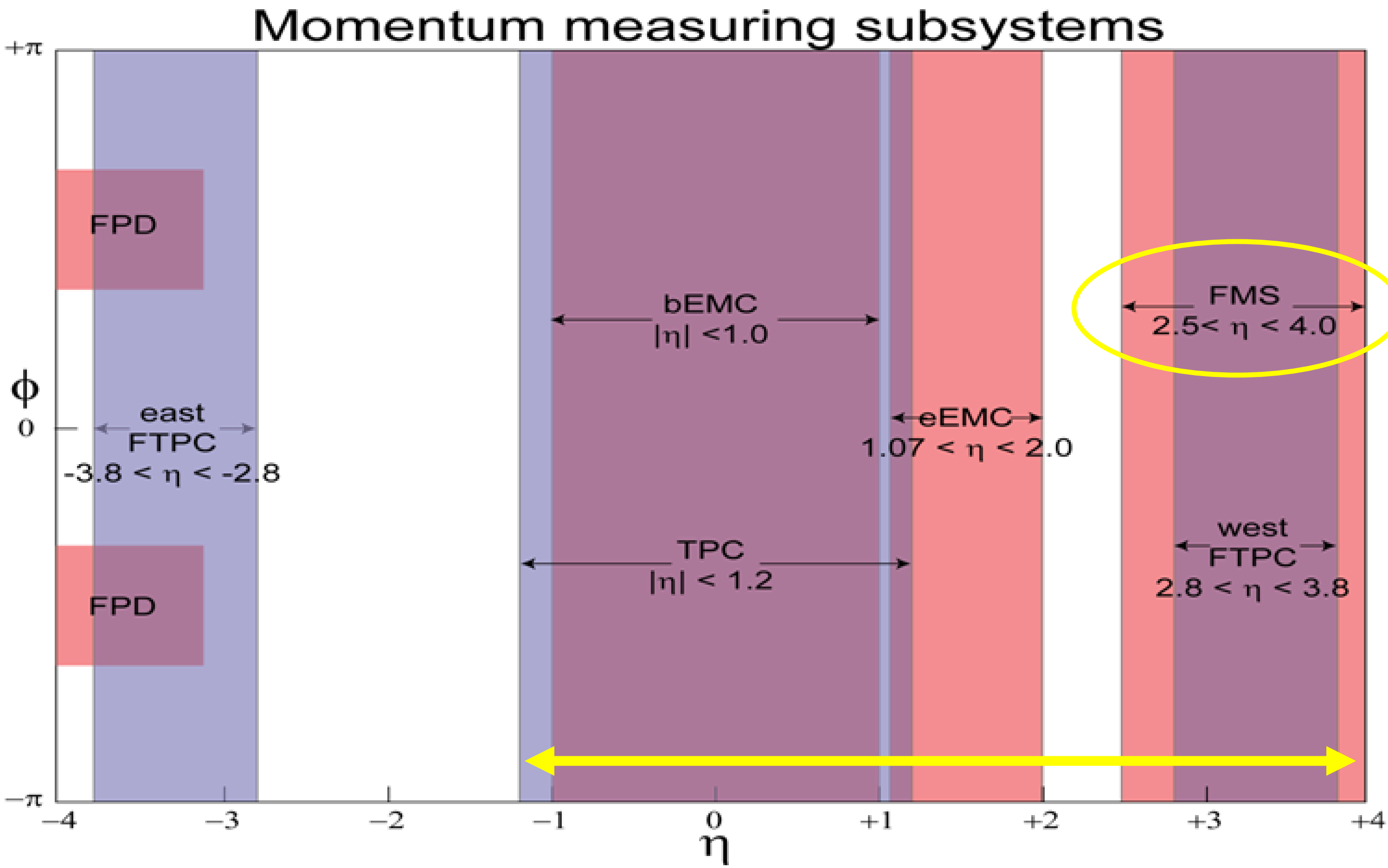


***FMS, EEMC and BEMC provides nearly complete EM coverage from $-1 \leq \eta \leq +4$***

# Lead Glass Cells



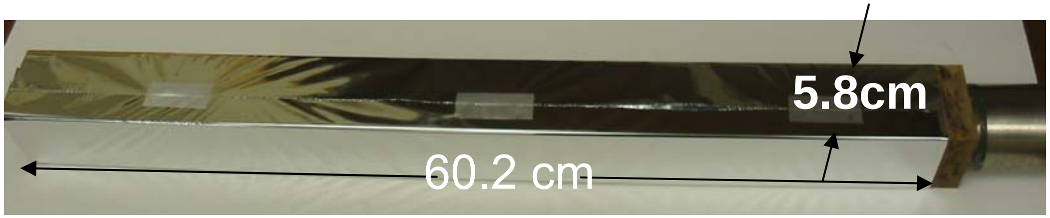


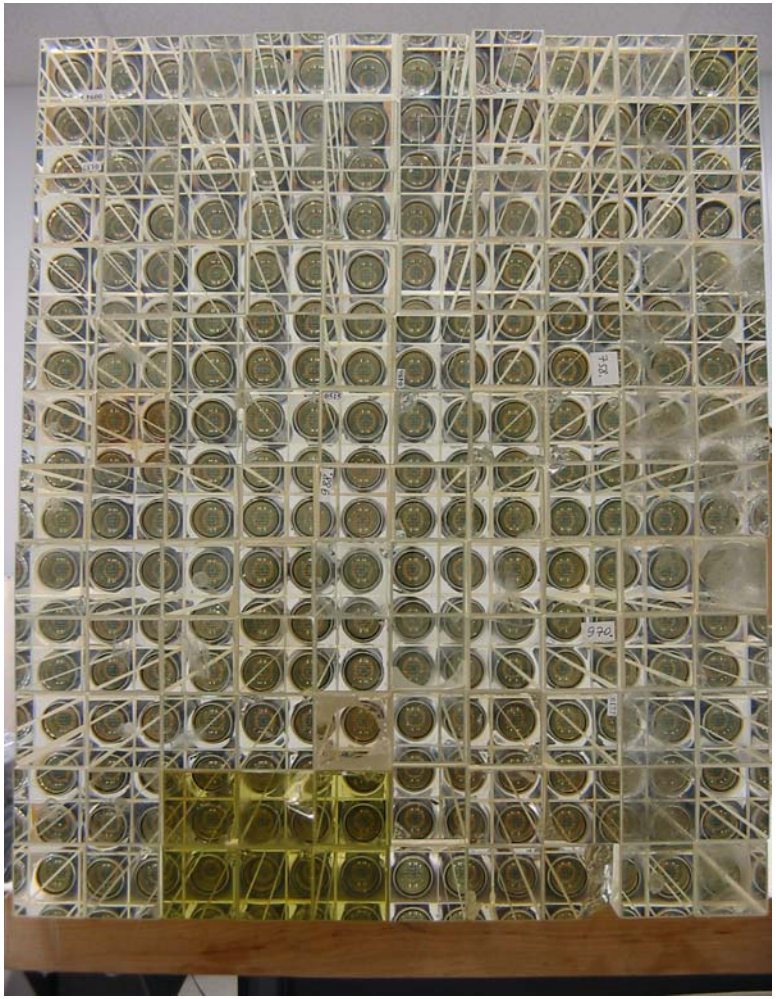

***Large Cells / 788 in Total***

From E831 at FNAL including
PMT's (XP2202) with resistive bases

$(5.8\text{cm})^2$ x 60.2 cm lead glass

18.75 radiation lengths

***Small Cells / 476 in total***

From IHEP Protvino including PMTs (FEU-84)
From JLab without PMTs
$(3.8\text{cm})^2$ x 45 cm lead glass
18 radiation lengths
Two types of PMTs: FEU84 and XP2972

# Outer Calorimeter HV system



***Large Cells***

All 788 large cells mate to XP2202 phototubes, powered by Zener-diode-stabilized resistive voltage dividers.

High-voltage delivered by four 256-channel LeCroy 1440 main frames

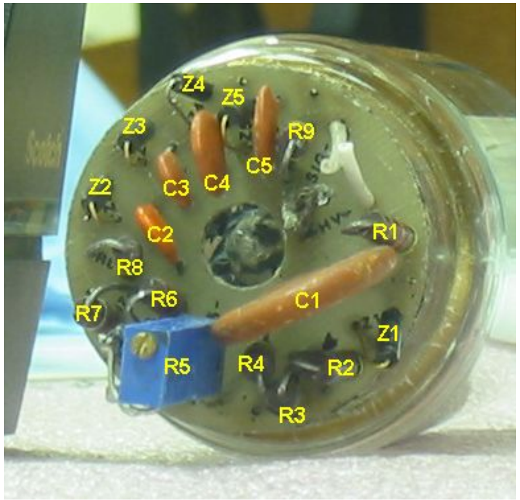

# Inner Calorimeter HV System

Steve Heppelman, Len Eun, et al. at Penn State University

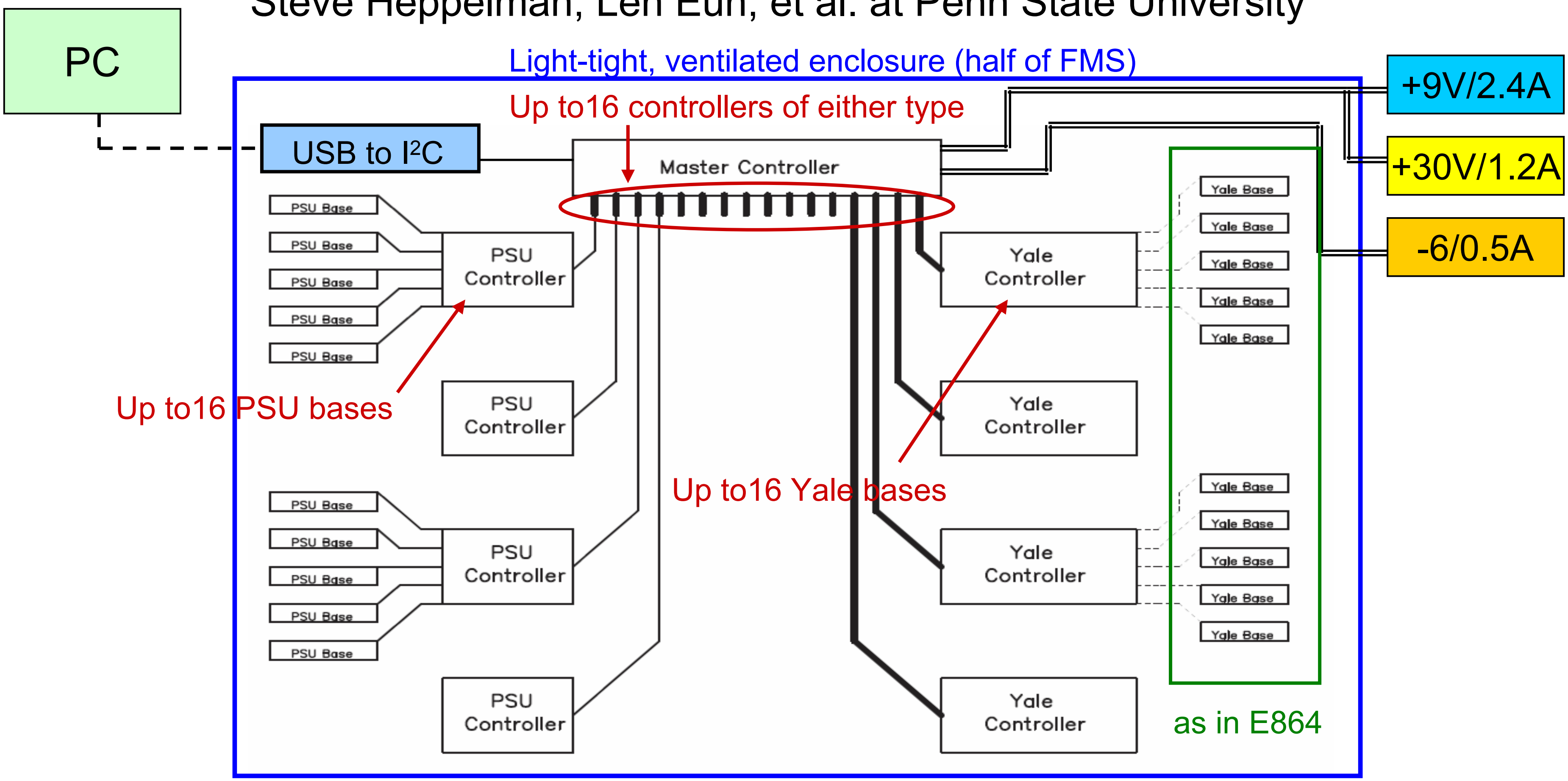


***PC-controlled 256-channel Cockcroft-Walton control systems***

# Inner Calorimeter HV System



Steve Heppelman, Len Eun, et al. at Penn State University

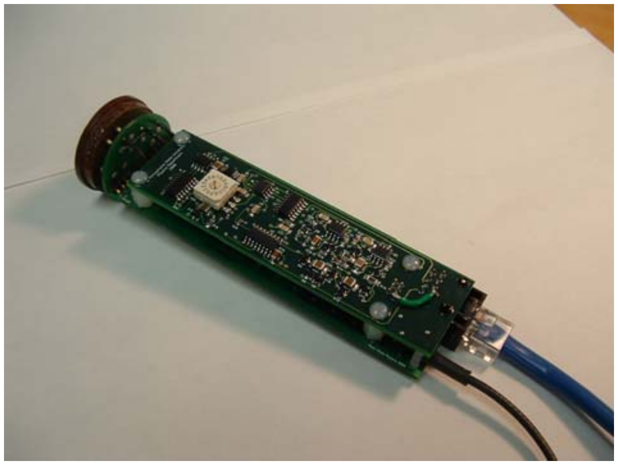

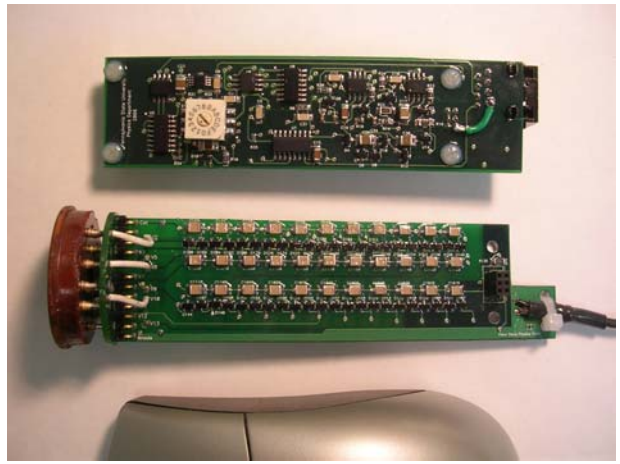

***Small Cell PSU Type***
***224 of 476***

Cockcroft-Walton HV bases with computer control through USB. Designed/built in house for FEU-84.

***Small Cell Yale Type***
***252 of 476***

XP2972 phototubes and bases **courtesy of Yale University**, from AGS-E864. Lacks digital control


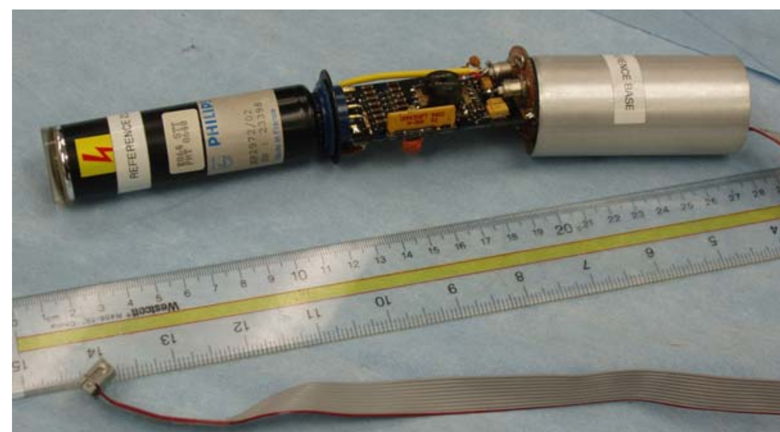

# Inner Calorimeter HV System



Steve Heppelman, Len Eun, et al. at Penn State University

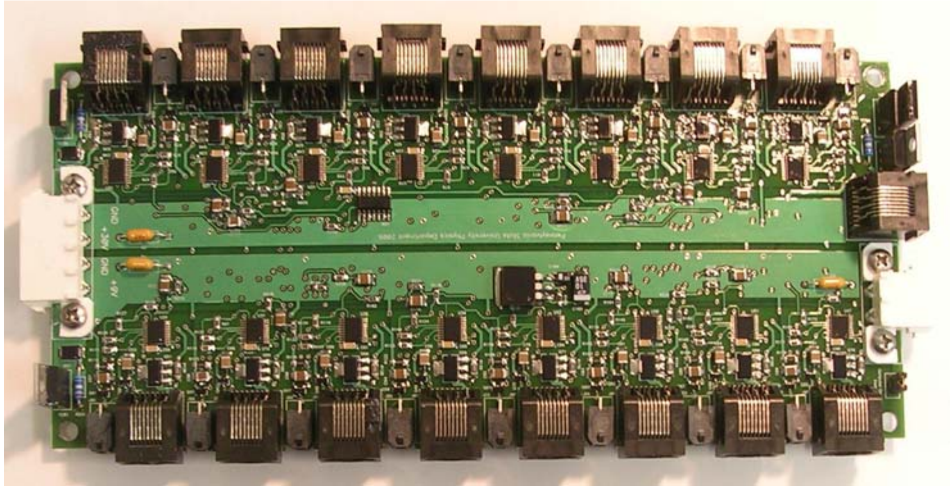

***Master Controller***

- Multiplexing up to 256 bases of either type.
- Voltage distribution
- Over voltage/over current protection

***'Yale' Controller***

- Provides computer control through USB to Yale Type cells.
- Voltage distribution
- Over current control

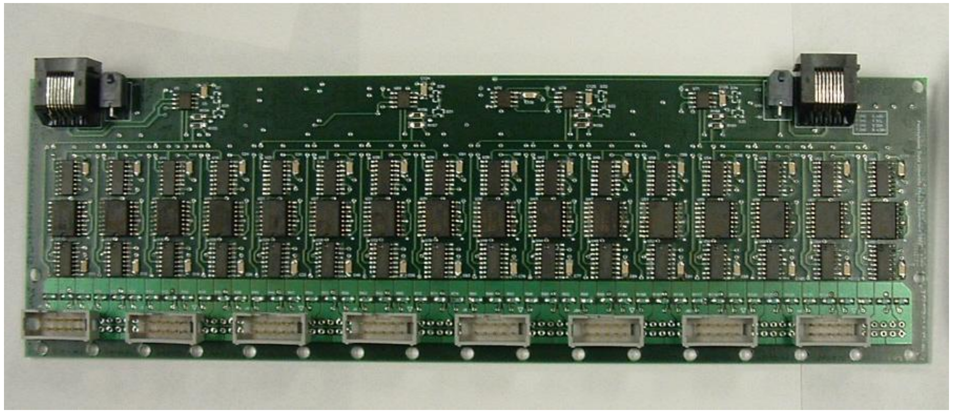

# Electronics and Trigger



Hank Crawford, Fred Bieser, Jack Engelage, Eleanor Judd, Chris Perkins, et al.
UC Berkeley/SSL

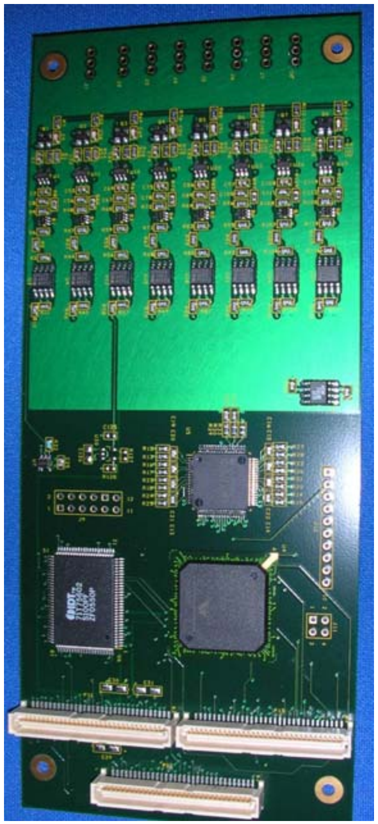

QT8 daughter card

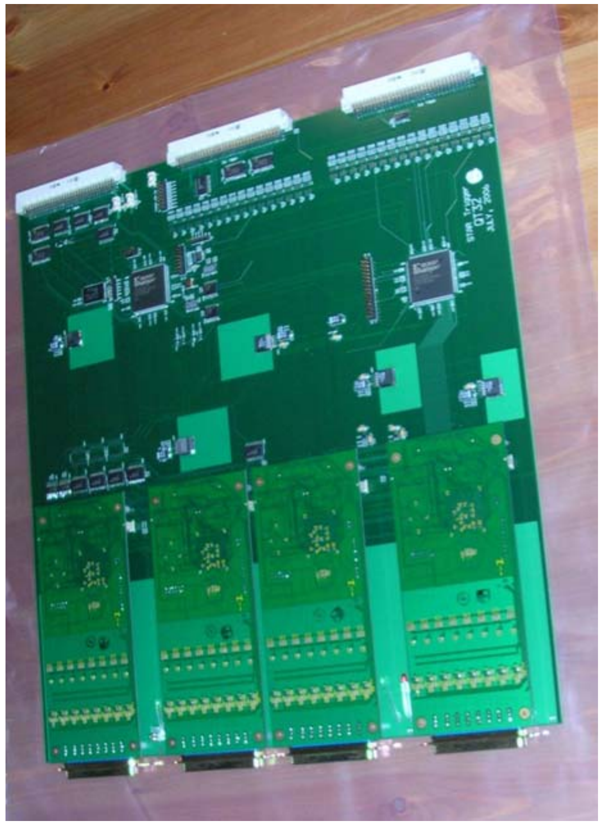

QT32 with 4 QT8 daughter cards

Readout of 1264 channels of FMS provided by QT boards. Each board has

- 32 analog inputs
- 12-bit ADC / channel
- 5-bit TDC / channel
- five FPGA for data and trigger
- operates at 9.38 MHz and higher harmonics
- produces 32 bits for each RHIC crossing for trigger

# Electronics and Trigger




***Present Status***

- 37/48 QT boards mounted in 9U VME in STAR Wide Angle Hall;
- all QT boards ready for installation;
- QT2,QT3,QT4 crates connected to phototubes and tested operational;
- Trigger connections completed; tests after run ends.

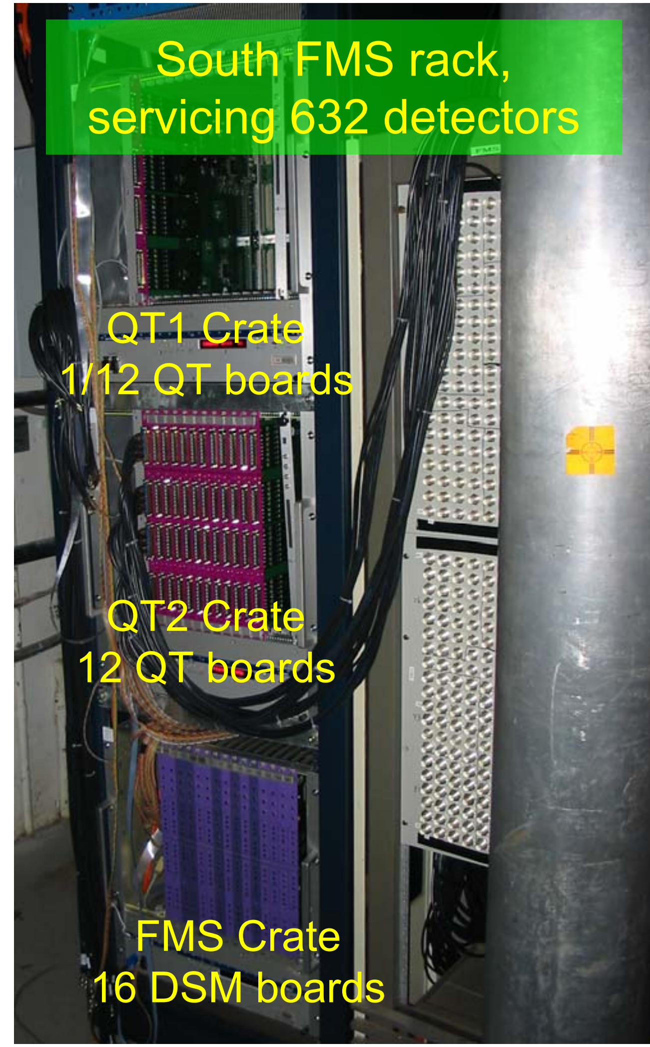

# FMS in Place



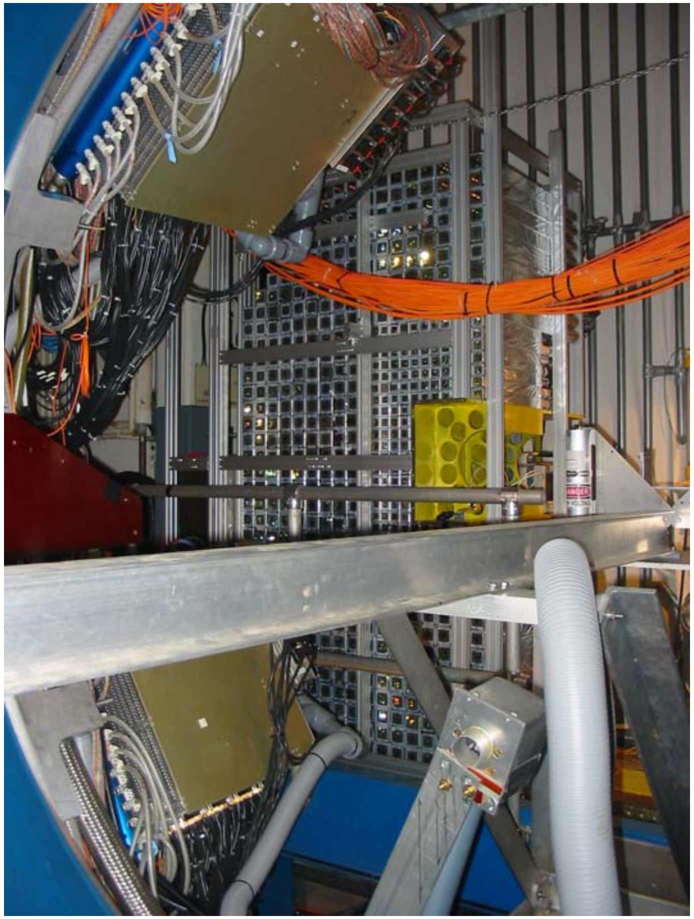

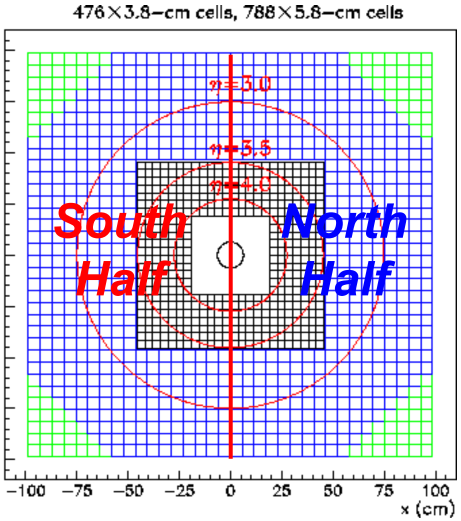


Detectors are stacked on the west platform in two movable halves.


South FMS half, as seen through the retracted west poletip.

(Partially stacked) North FMS half, positioned close to the beam pipe.

# Commissioning of FMS During Run7



## Au Au FMS Commissioning

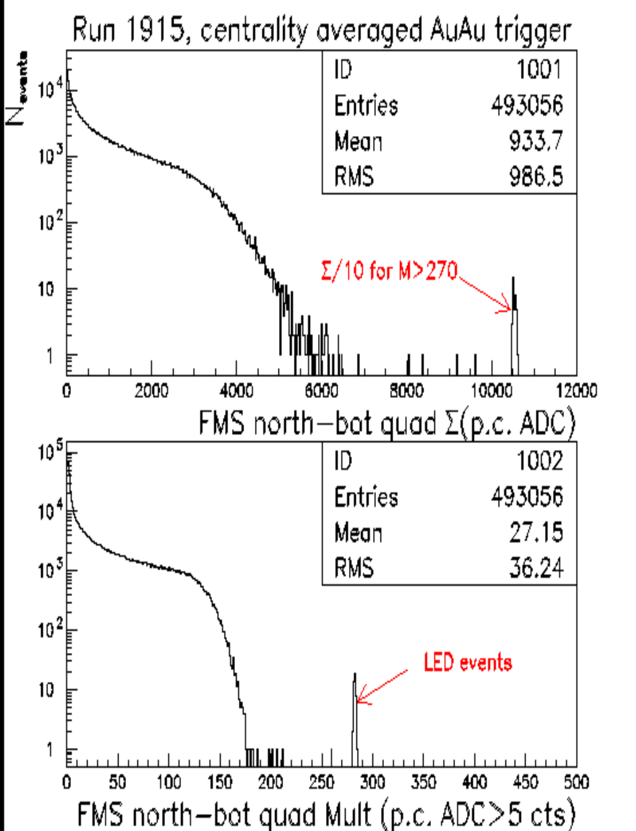


***Ready for Production Now and in Run8***

***COMPLETED***

- Cell-by-cell scans of HV to check HV and signal connections
- Quadrant-by-quadrant total-energy measurements
- Initial timing for QT electronics

Summed Energy (ADC cnts)

Cell multiplicity

QT gate →

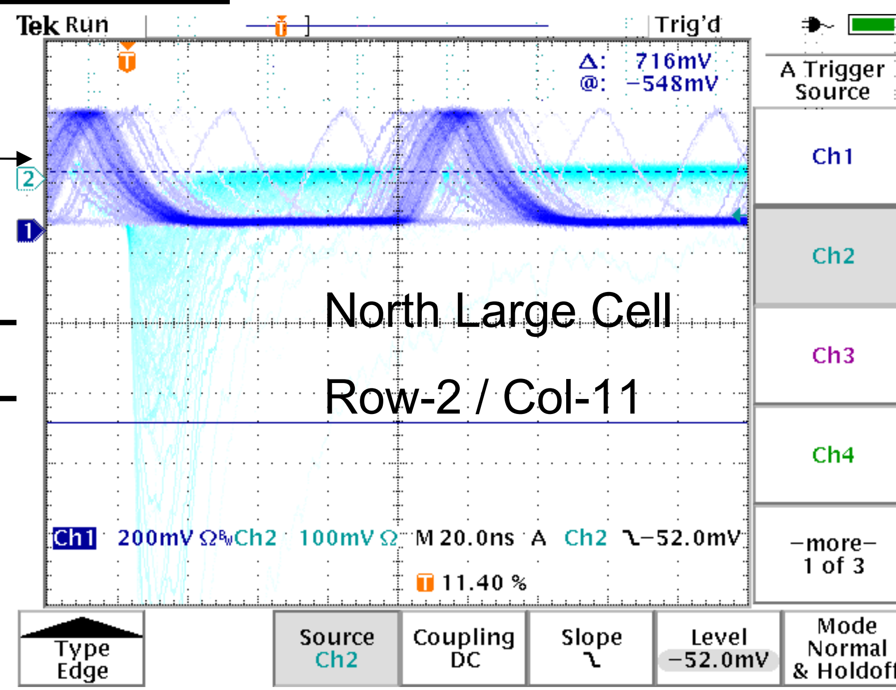




PENNSTATE 1855

# STAR FMS Proposal Highlights



**[hep-ex/0502040]**

F. Bieser[2], L. Bland[1], R. Brown[1], H. Crawford[2], A. Derevshchikov[4], J. Drachenberg[5], J. Engelage[2], L. Eun[3], C. Gagliardi[5], S. Heppelmann[3], E. Judd[2], V. Kravtsov[4], Yu. Matulenko[4], A. Meschanin[4], D. Morozov[4], L. Nogach[4], S. Nurushev[4], A. Ogawa[1], C. Perkins[2], G. Rakness[1,3], K. Shestermanov[4], and A. Vasiliev[4]

[1] Brookhaven National Laboratory
[2] University of Berkeley/Space Sciences Institute
[3] Pennsylvania State University
[4] IHEP, Protvino
[5] Texas A&M University

1. A **$d(p)+Au \rightarrow \pi^0\pi^0+X$** measurement of the **parton model gluon density distributions *xg*(*x*)** in **gold nuclei** for **0.001< *x* <0.1**. For 0.01<*x*<0.1, this measurement tests the universality of the gluon distribution.

   } DOE milestone

2. Characterization of correlated pion cross sections as a function of $Q^2$ ($p_T^2$) to search for the onset of **gluon saturation effects** associated with **macroscopic gluon fields. (again d-Au)**

3. Measurements with **transversely polarized protons** that are expected to **resolve the origin of the large transverse spin asymmetries** in reactions for **forward $\pi$0 production. (polarized pp)**

# Back up

# Forward $\pi^0$ Cross Section at STAR

hep-ex/0505024

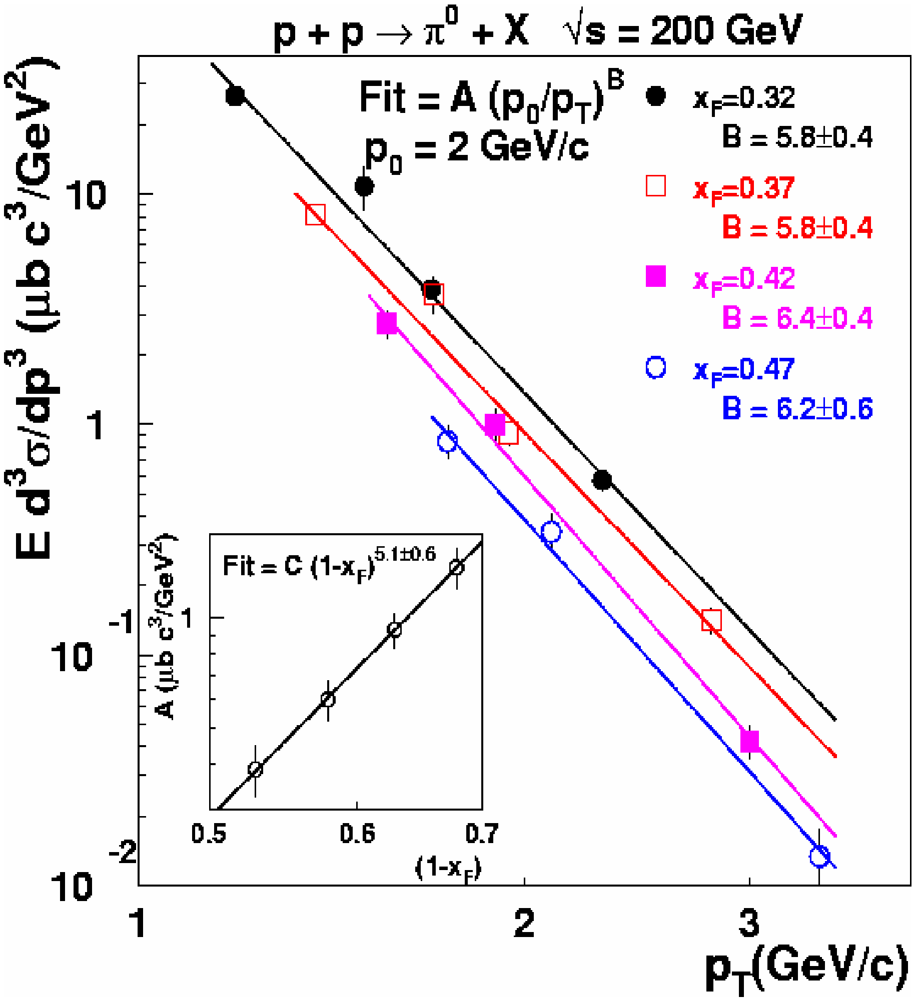


Unpolarized forward $\pi^0$ cross section shows power law dependence on $p_T$ at fixed $x_F$, and $(1 - x_F)$ at fixed $p_T$.

$$E\frac{d^3\sigma}{dp^3} \propto (1-x_F)^N p_T^{-B}$$

$$N \approx 5$$

$$B \approx 6$$

Similar to ISR analysis

J. Singh, et al Nucl. Phys. B140 (1978) 189.

# Average $x_F$ in $p_T$ bins

**$0.25 < x_F < 0.30$**

| $p_T$ bin | $\langle p_T \rangle$, GeV/c | $\langle x_F \rangle$ |
|---|---|---|
| 0.5-1.1 | 0.95 | 0.273 |
| 1.1-1.4 | 1.26 | 0.282 |
| 1.4-1.9 | 1.61 | 0.278 |
| 1.9-2.4 | 2.10 | 0.273 |
| 2.4-5.0 | 2.53 | 0.284 |

**$0.30 < x_F < 0.35$**

| $p_T$ bin | $\langle p_T \rangle$, GeV/c | $\langle x_F \rangle$ |
|---|---|---|
| 0.5-1.2 | 1.06 | 0.321 |
| 1.2-1.7 | 1.47 | 0.322 |
| 1.7-2.2 | 1.87 | 0.330 |
| 2.2-2.7 | 2.41 | 0.323 |
| 2.7-5.0 | 2.85 | 0.330 |

**$0.35 < x_F < 0.40$**

| | | |
|---|---|---|
| 0.5-1.5 | 1.29 | 0.368 |
| 1.5-1.9 | 1.70 | 0.370 |
| 1.9-2.4 | 2.08 | 0.374 |
| 2.4-3.0 | 2.64 | 0.373 |
| 3.0-5.0 | 3.18 | 0.377 |

**$0.40 < x_F < 0.47$**

| | | |
|---|---|---|
| 0.5-1.7 | 1.45 | 0.423 |
| 1.7-2.2 | 1.94 | 0.426 |
| 2.2-2.7 | 2.38 | 0.433 |
| 2.7-3.3 | 2.94 | 0.430 |
| 3.3-5.0 | 3.54 | 0.435 |

# Expanding Forward Calorimeter

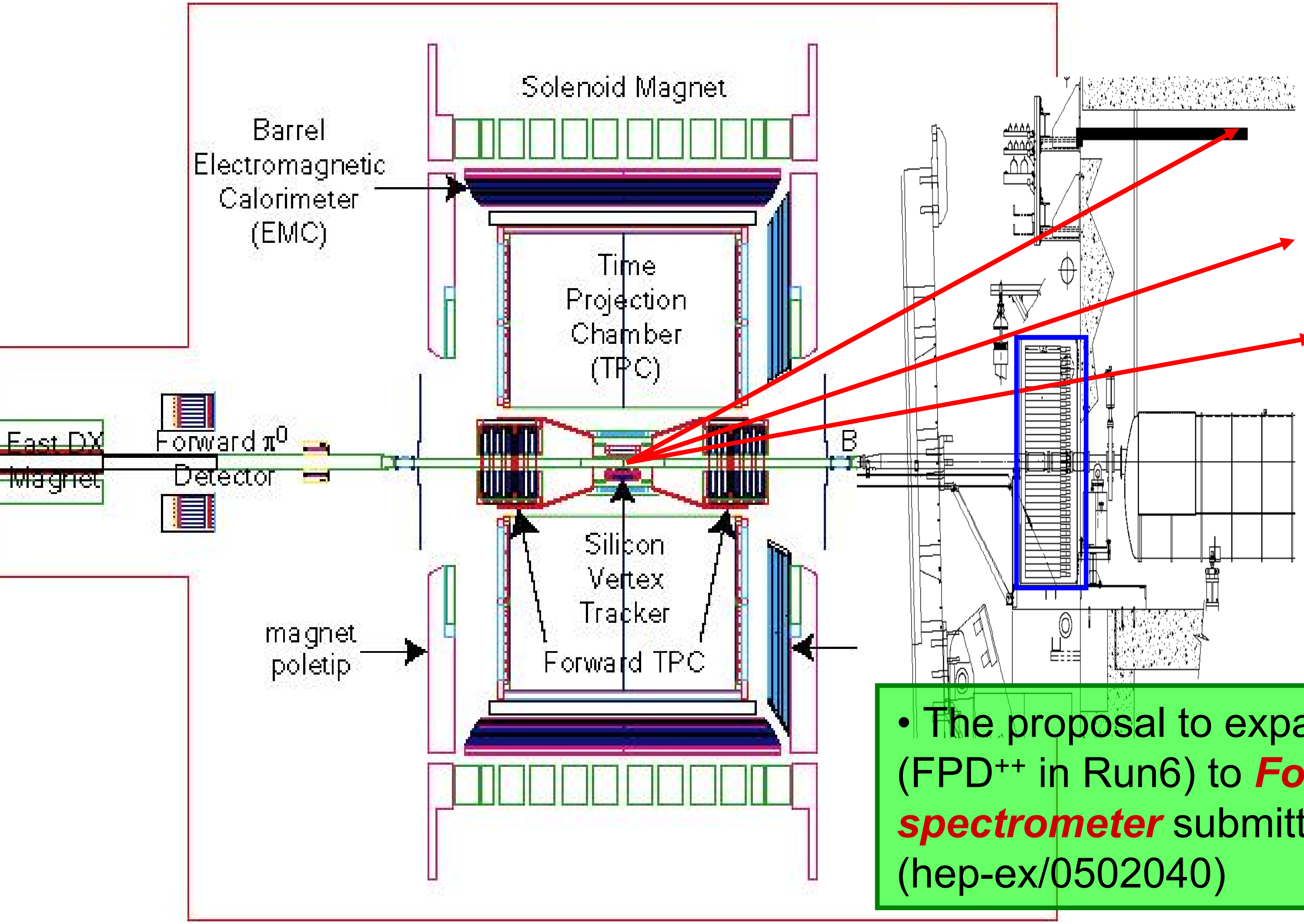


- The proposal to expand the west FPD ($FPD^{++}$ in Run6) to ***Forward Meson spectrometer*** submitted in Feb. 2005 (hep-ex/0502040)